4,5-Dihydro-1*H*-pyrazole Derivatives with Inhibitory nNOS Activity in Rat Brain: Synthesis and Structure−Activity Relationships

M. Encarnación Camacho,[†] Josefa León,[‡] Antonio Entrena,[†] Guillermo Velasco,[†] M. Dora Carrión,[†] Germaine Escames,[‡] Antonio Vivó,[§] Darío Acuña-Castroviejo,[‡] Miguel A. Gallo,[†] and Antonio Espinosa*[,1]

Departamento de Química Farmacéutica y Orgánica, Facultad de Farmacia, Universidad de Granada, Spain, Departamento de Fisiología. Instituto de Biotecnología, Universidad de Granada, Spain, and Hospital Costal del Sol, Marbella (Málaga), Spain

Received January 15, 2004

In an attempt to find new compounds with neuroprotective activity, we have designed, synthesized and characterized 19 new nNOS inhibitors with a 4,5-dihydro-*1H*-pyrazole structure. Compounds **11r** [1-cyclopropanecarbonyl-3-(2-amino-5-chlorophenyl)-4,5-dihydro-*1H*-pyrazole] and **11e** [1-cyclopropanecarbonyl-3-(2-amino-5-methoxyphenyl)- 4,5-dihydro-*1H*-pyrazole] show the highest activities with inhibition percentages of 70% and 62%, respectively. A structure−activity relationship for the nNOS inhibition can be established from the structural comparison of these new pyrazole derivatives and the described synthetic kynurenines **10**.

Introduction

Glutamate is a very important neurotransmitter that controls several functions in the central nervous system (CNS). It is the main excitatory signaling mediator, and it is implicated in functions such as memory and learning. Nevertheless, glutamate can also produce neurotoxicity, and consequently, the glutamate homeostasis must be carefully regulated.[1] *N*-Methyl-D-aspartate (NMDA) receptors are a subtype of glutamate receptors that, upon activation by glutamate, produce a Ca^{2+} influx into the neuronal cell among other ions such as Na^+ and K^+.[2] An overstimulation of the NMDA receptors produces an accumulation of intracellular Ca^{2+} that in turn activates a series of enzyme like lipases, proteases, and nitric oxide synthase (NOS), leading to the formation of reactive oxygen species (ROS), responsible of the neuronal damage.[3−5]

The kynurenine metabolic pathway of L-tryptophan in the brain turn out to be of great interest in neuroprotection because kynurenic and quinolinic acids, two intermediate metabolites of this pathway, modulate the NMDA receptor in a functionally opposite manner.[6−9] Quinolinic acid **1** is a selective agonist of the NMDA binding site at the NMDA receptor[10] and is a potent neurotoxin[11−16] while kynurenic acid **2** is a nonselective antagonist of the glycine$_B$ recognition site at the NMDA receptor[17,18] and has neuroprotective properties.[19−21] Kynurenic acid has been used as a template in the design and development of selective therapeutic agents structurally related to kynurenines and with higher NMDA antagonistic properties. This approximation has become a very important strategy to reduce the overstimulation of the NMDA receptor[21−26] and to produce neuroprotection, and 7-chlorokynurenic acid **3**[22] and 5,7-dichlorokynurenic acid **4**[23] are very well-known examples of compounds designed by this strategy. Compound ZD9379 **5** produces neuroprotection in rats 24 h after administration.[24] Nevertheless, although many of these compounds demonstrate efficacy in animal models of ischemia, they do not prevent neuronal damage in human after ischemia, probably due to the wide variability of the cerebral damage in human beings.[25]

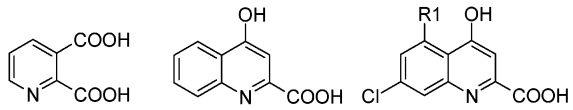

1 2 3: R1 = H 4: R1 = Cl

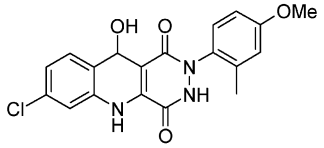

5: ZD9379

A second strategy in order to produce neuroprotection is to increase the endogenous kynurenic acid production through the inhibition of key enzymes in the brain kynurenine pathway.[26] The inhibition of the kynurenine 3-hydroxylase (KYN3OH) produces a reduction of both neurotoxic quinolinic acid **1** and 3-hydroxykynurenine **6** and consequently increase the biosynthesis of kynurenic acid **2**. Nicotinylalanine **7**[27] was the first competitive inhibitor of this enzyme that is able to increase the kynurenic acid level in brain showing anticonvulsant properties.[28] Several other kynurenine 3-hydroxylase inhibitors have been synthesized, and UPF648 (**8**) is the most potent one reported to date.[29]

Nitric oxide (NO) is a well-known biologically active compound that acts as cell messenger with important regulatory functions in the nervous, immune, and cardiovascular systems.[30] In mammals, NO is synthesized from L-arginine in various cell types (neurons,[31] endothelial cells,[32] and macrophages[33,34]) by a family of

* To whom correspondence should be addressed: Dr. Antonio Espinosa Ubeda. Dpto. Química Farmacéutica y Orgánica. Facultad de Farmacia. Universidad de Granada. 18071 Granada (Spain). Phone: +34-958-243850, Fax: +34-958-243845, E-mail: aespinos@ugr.es.

[†] Departamento de Química Farmacéutica y Orgánica.

[‡] Departamento de Fisiología.

[§] Hospital Costal del Sol.

10.1021/jm0407714 CCC: $27.50
Published on Web 10/01/2004

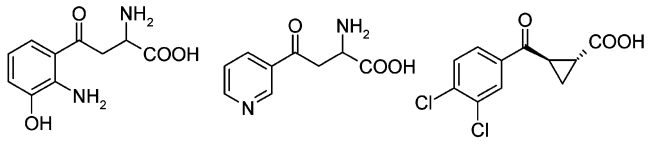

6 7 8: UPF648

nitric oxide synthase (NOS) isoenzymes.[35,36] The constitutive endothelial (eNOS) and neuronal (nNOS) isoforms are calcium/calmoduline dependent and are physiologically activated by hormones or neurotransmitters that increase the intracellular calcium concentration. In contrast, the inducible iNOS isoform is activated by basal intracellular calcium concentrations, and, once expressed, it remains permanently activated, yielding high NO concentrations. This mechanism is part of the normal immune response against invading pathogens and neoplasic cells.[37] Although NO is not involved in the synaptic transmission under normal conditions, an excessive NO production by some of the NOS-isoenzymes may be detrimental. Thus, it is well-known that an overproduction of NO produces neurotoxicity, and this fact has been associated with several neurological disorders such as Alzheimer's disease,[38,39] amyotrophic lateral sclerosis,[40] and Huntington's disease.[41] For this reason, a third and recent strategy in the development of successful neuroprotective agents is orientated toward the synthesis of new structures that interfere with some step of the complex chemical signaling system involving NOS, including the inhibition of the enzyme itself. It has been shown that melatonin **9**, the main compound secreted by the pineal gland, can inhibit the nNOS activity in rat striatum in a dose-dependent manner.[42]

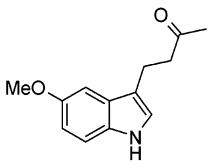

9

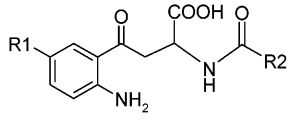

10a, R_1=OCH_3, R_2=Me
10b, R_1=OCH_3, R_2=Pr

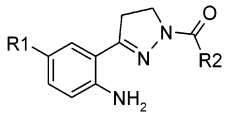

11

Recently, we have synthesized and evaluated a series of kynurenine derivatives; among them, **10a** and **10b** showed a significant nNOS inhibitory activity.[42,43] In these compounds, the side chain conformational mobility is restricted by the formation of an intramolecular hydrogen bond between both the 2-NH_2 and the carbonyl ketonic groups, and as a consequence of this restriction, the kynurenine derivative can mimic the active conformation of melatonin **9** when it interacts with its biological target.[43] Nevertheless, both structures **9** and **10** are still quite flexible, and they could adopt several conformations.

In this paper we describe a new type of nNOS inhibitor of general formula **11**, bearing a 4,5-dihydro-1*H*-pyrazole fragment, that shows a good inhibitory activity and could be used as a template in the development of new neuroprotectors agents. To confirm that their potential neuroprotective activity is due to the nNOS inhibition, we have also tested all these compounds as well as the kynurenines **10a** and **10b** as inhibitors of the KYN3OH, showing that all compounds are inactive against this enzyme.

Chemistry. Scheme 1 represents the general synthetic pathway for all the final 4,5-dihydro-1*H*-pyrazole derivatives described in this paper. In general, two modifications in the structure were performed in order to modulate the potency: (i) modification of the lateral amide chain in the pyrazole ring, and (ii) substitution on the benzene C-5 atom. Depending on the C-5 substituents, the studied compounds can be classified in three series: series A (R_1 = OMe, compounds **11a**−**i**), series B (R_1 = H, compounds **11j**−**n**), and series C (R_1 = Cl, compounds **11o**−**s**). Commercially available 2-nitrobenzaldehyde **12b** or 5-chloro-2-nitrobenzaldehyde **12c** were used for the synthesis of series B and C, respectively. 5-Methoxy-2-nitrobenzaldehyde **12a** was synthesized from 5-hydroxy-2-nitrobenzaldehyde by reaction with MeI in the presence of K_2CO_3/THF[44] and used as the precursor of all compounds belonging to series A. Reactions of compounds **12a**−**c** with vinylmagnesium bromide quantitatively yield the corresponding allylic alcohols **13a**−**c**, which were further oxidized (Jones reagent) to obtain the corresponding enones **14a**−**c** (80% yield).[45]

Reaction of the enones **14a**−**c** with hydrazine in ethanol produces the corresponding 4,5-dihydro-1*H*-pyrazoles **15a**−**c**, which are acylated in situ by treatment with acetic anhydride or with the corresponding acyl chloride to obtain the 1-acyl-3-(2-nitro-5-substituted-phenyl)-4,5-dihydro-1*H*-pyrazoles **16a**−**s**. The overall yield of these reactions vary from 50% to 90% and depends on both R_1 and R_2 substituents, being smaller for series C than for series A or series B. In general, acetyl and benzoyl derivatives give the lower and higher yields of each series, respectively. Finally, reduction of the aromatic nitro group leads to the final compounds **11a**−**s** in a quantitative manner. The reduction of both series A and B was carried out by catalytic hydrogenation (Pd/C), while in series C reduction was accomplished by reaction with $SnCl_2$ (1:5 molar ratio) in order to avoid dechlorination.

Molecular Modeling and Conformational Analysis. The conformational analysis of the 4,5-dihydro-1*H*-pyrazole **11j** (the simplest of all compounds) indicates the existence of four different conformers. Figure 1 shows these conformations as well as their relative energies calculated by means of both Tripos force field[46] and ab initio calculations (Gaussian98,[47] 6-31G*), both methods indicating a similar order in stability.

The greater stability of conformers **I** and **II** is due to two structural aspects: (i) The existence of a hydrogen bond between the 2′-NH_2 group and the N-2 nitrogen of the pyrazoline ring that stabilizes both conformers and that cannot be formed in conformers **III** and **IV** due to the inappropriate orientation of the pyrazole ring. (ii) The stabilization due to the conjugation between the C=N double bond and the benzene ring. On the contrary, the steric interactions between the 2′-NH_2 group and the hydrogen atoms of the C-4 pyrazole in conformers **III** and **IV** seem to be strong enough to prevent the

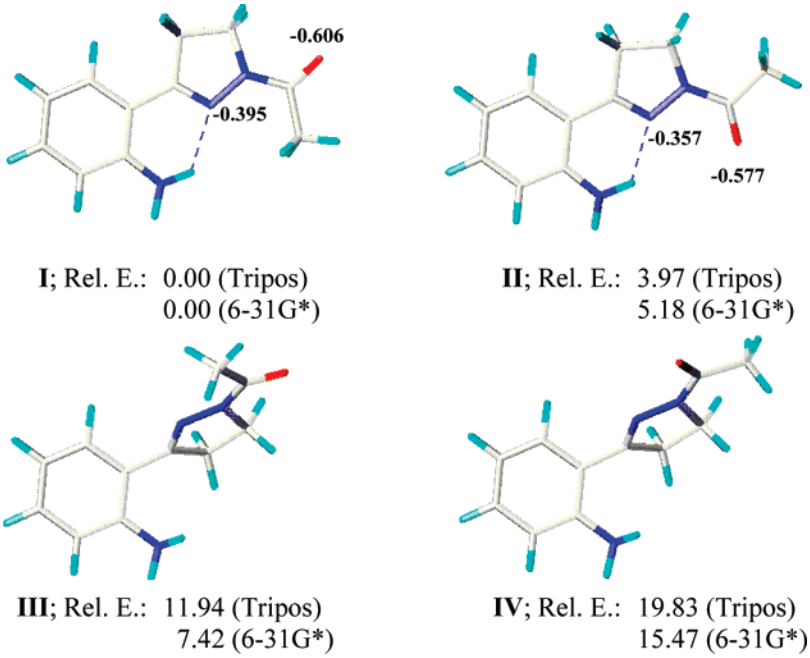

Figure 1. The four main conformations found for compound **11j.** Relative energies calculated by molecular mechanics (Tripos) or by ab initio (6-31G*) calculations are expressed in kcal/mol. Partial atomic charges (ab initio) calculated for both the carbonyl O atom and the N-2 pyrazole atom are shown for conformations **I** and **II**. Blue lines represent the intramolecular hydrogen bond present in conformers **I** and **II**. It can also be observed the lack of coplanarity in **III** and **IV** due to steric interactions between the NH_2 and CH_2 groups.

Scheme 1

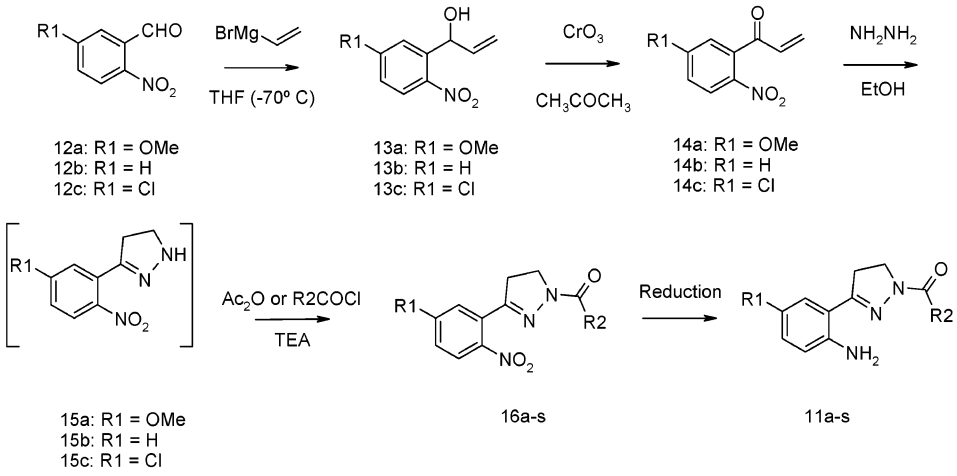

coplanarity of both rings and to soften the conjugation. On the other hand, the difference in energy between conformers **I** and **II** seems to be associated to the electrostatic interactions between the oxygen carbonyl group and the N-2 atom. Both atoms bear a significant negative charge (Figure 1), and strong electrostatic repulsions arise from the proximity of both atoms in the conformation **II** if compared with the most stable conformer **I**.

Compounds of series A and C also show a similar conformational behavior. The presence of the chlorine atom (series C) has only a minor influence in the energy differences among the different conformations (data not shown). In series A, the methoxy group allows the existence of different rotamers for each conformer due to the rotation around the C−O bond. This fact increases the total number of conformations in this family compared with those of series B and C, but it does not significantly affect the overall conformational behavior since rotation around the C−O bond can take place very easily. Nevertheless, all conformers of series A and C can be classified within one of the four conformations previously described for series B.

The energy difference between the four described conformations is high enough to consider that conformer **I** is the only one present in solution. In fact, compound **11*l*** (R_1 = H, R_2 = Pr) shows NOE effects in ^{1}H NMR spectroscopy between the H-6′ benzene atom and hydrogen atoms of the C-4 pyrazole atom and between the NH_2 group and both CH_2 groups. These NOE effects are compatible only with the existence in solution of a conformation for compound **11*l*** similar to the conformer **I**.

Results and Discussion

In a previous paper[43] we have described the effects of several kynurenine derivatives of general structure **10** on the excitatory response of striatal neurons to

SMCx stimulation, an experimental paradigm involving the activation of the NMDA subtype of glutamatergic receptor. Among such compounds, two of them (**10a** and **10b**) show strong inhibitory effect on the striatal excitatory response and are characterized by the presence of a 2-NH_2 group on the benzene ring. Removing this group provokes a significant decrease in the inhibitory response. Our previous results indicate that there was no response when these compounds were iontophoretized onto a silent neuron in absence of NMDA ejection,[43] thus suggesting that they act by reducing the excitatory response elicited by NMDA activation. Compounds **10a** and **10b** are also able to significantly reduce the nNOS activity while all other compounds do not show similar nNOS inhibitory activity.[43]

Here we have also tested the kynurenines **10a** and **10b** as inhibitors of the KYN3OH. The most interesting result from these experiments is that compounds **10a** and **10b** do not show any inhibitory activity against this enzyme. Since both compounds are able to inhibit both the NMDA-dependent excitability and nNOS activity, it can be concluded that their inhibitory properties are only due to the nNOS inhibition. Compounds **10a** and **10b** bear a 2′-NH_2 group on the benzene ring, and this feature seems to be necessary for the nNOS inhibition. Two reasons can be argued to justify the importance of this group and its influence in the inhibition of nNOS. On one hand, the 2′-NH_2 group forms a strong intramolecular hydrogen bond with the carbonyl moiety, restricting the conformational mobility and allowing the side chain to mimic melatonin, a known nNOS inhibitor.[42] On the other hand, it seems that the additional NH bond of the 2′-NH_2 group can form another hydrogen bond with some critical residues of nNOS when the complex is formed.[43]

Following these reasoning, we have designed and synthesized the new class of nNOS inhibitors described in this paper, the 4,5-dihydro-1*H*-pyrazole derivatives, that can be considered as rigid analogues of the synthetic kynurenines previously described: (i) these new compounds bear the 2′-NH_2 group in the benzene ring that forms the intramolecular hydrogen bonds with the pyrazole N-2 atom and also can rise to a favored interaction with the enzyme, (ii) the presence of the pyrazole ring confers higher rigidity to the molecule as has been described previously in the conformational analysis of these compounds, and (iii) the final amide group is also present in these molecules, being the nitrogen atom part of a rigid and delocalized π-system.

Table 1 and Figure 2 illustrate both the nNOs inhibition and KYN3OH activity in the presence of 1 mM concentration of each pyrazoline. Only compounds **11j** and **11b** (with inhibitions of 22.15% and 18.86%, respectively) are very weak inhibitors of KYN3OH, and results obtained for the rest of compounds are not statistically significant.

By contrast, all compounds show good nNOS inhibiton, depending on the substitution on both R_1 and R_2 groups. From a qualitative point of view, the influence of R_2 over the activity seems to be clear since, in general, it can be observed that an increment in the volume of R_2 increases the inhibitory activity. Thus, the change of Me group by Et increases the activity in the three series, cyclopropyl is the better inhibitor in series A and C, the phenyl group gives rise to high inhibition in all series, and cyclohexyl also gives good inhibition in series

Table 1. Structure and Biological Activities of Kynurenine **10a**,**b** and 4,5-Dihydro-1*H*-pyrazole Derivatives **11a**−**s**. R_1 Defines the Series A (R_1 = OMe), B (R_1 = H), and C (R_1 = Cl)

compd	R_1	R_2	% nNOS inhibition[a]	% kynurenine 3-hydroxylase activity[b]
10a	OCH_3	Me	68.49 ± 9.92[c]	100.52 ± 9.7
10b	OCH_3	Pr	45.05 ± 8.56[c]	88.72 ± 10.2
11a	OCH_3	Me	38.04 ± 1.53	98.84 ± 11.3
11b	OCH_3	Et	53.27 ± 2.83	81.14 ± 8.6
11c	OCH_3	Pr	34.70 ± 1.32	96.43 ± 10.6
11d	OCH_3	Bu	49.76 ± 1.53	120.50 ± 12.3
11e	OCH_3	c-C_3H_5	62.24 ± 4.68	123.35 ± 11.1
11f	OCH_3	c-C_4H_7	38.30 ± 3.33	96.54 ± 9.07
11g	OCH_3	c-C_5H_9	49.87 ± 4.13	105.19 ± 10.1
11h	OCH_3	c-C_6H_{11}	62.20 ± 1.91	87.36 ± 7.9
11i	OCH_3	Ph	58.92 ± 3.55	*d*
11j	H	Me	33.69 ± 3.62	77.85 ± 8.6
11k	H	Et	36.47 ± 4.52	85.25 ± 7.8
11*l*	H	Pr	52.39 ± 2.24	84.95 ± 7.9
11m	H	c-C_3H_5	38.79 ± 3.18	86.93 ± 9.4
11n	H	Ph	57.05 ± 3.13	82.46 ± 9.9
11o	Cl	Me	47.58 ± 4.01	110.59 ± 10.5
11p	Cl	Et	46.15 ± 5.66	97.74 ± 11.1
11q	Cl	Pr	34.43 ± 3.70	97.74 ± 10.2
11r	Cl	c-C_3H_5	70.24 ± 5.60	98.12 ± 10.1
11s	Cl	Ph	61.12 ± 3.11	105.71 ± 9.5

[a] Data represent the mean ± SEM of the percentage of nNOS inhibition produced by 1 mM concentration of each compound. Each value is the mean of three experiments performed by triplicate in homogenates of four rat striata in each one. [b] Data represent the mean ± SEM of the KYN3OH activity in the presence of 1 mM concentration of each compound. [c] See ref 44. [d] Not tested.

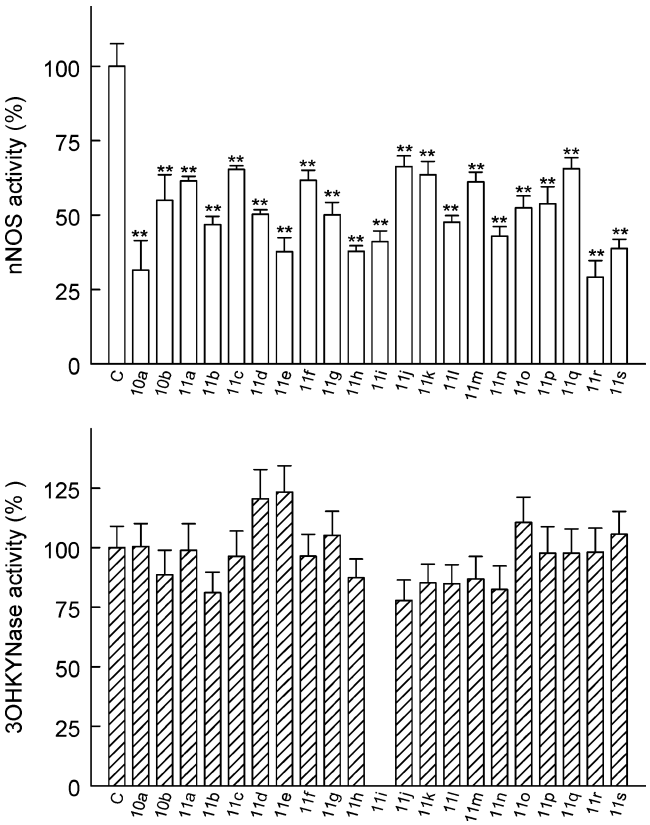

Figure 2. Percent of nNOS (top) and KYN3OH (bottom) activities in the presence of 1 mM concentration of each compound as compared with untreated samples (C). Each value is the mean of three experiments performed by triplicate in homogenates of four rat striata in each one. $^{**}P > 0.01$ vs control.

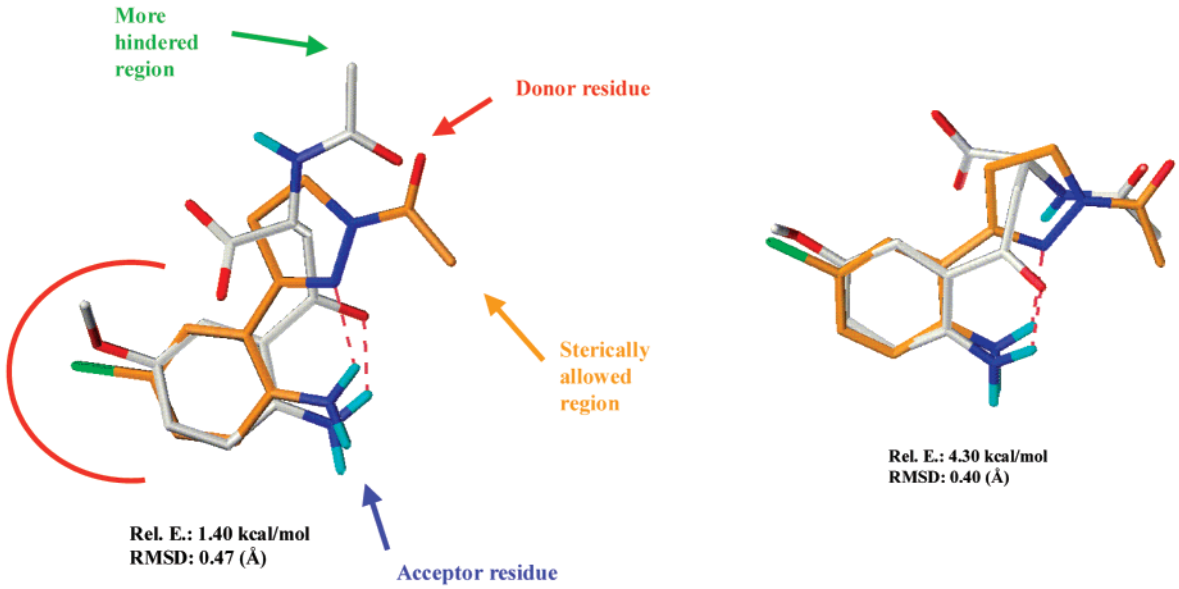

Figure 3. Superimposition of corresponding conformations of compounds **10a** (color by atoms) and compound **11o** (carbon atoms colored in orange). Relative energies correspond to the **10a** conformation and RMSD indicates the goodness of the superimposition considering the aromatic ring, the NH_2 group, and the amide oxygen atom as fitting atoms. The red arc indicates the hydrophobic pocket of the benzene ring. Blue and red arrows indicate the interaction with the hydrogen bond acceptor and donor residues, respectively. Pocket for accommodation of the R_2 amide substituent are indicated by the green (kynurerine) and orange (pyrazole) arrows.

A. In relation to R_1, it can be observed that compounds belonging to series A (R_1 = OMe) or C (R_1 = Cl) are more active than those of series B (R_1 = H). Only compound **11*l*** (R_2 = Pr), belonging to series B, shows higher activity than the corresponding one of the other series. Unfortunately, we have not found any quantitative relationships between the volume of the substituent R_2 or the nature of R_1 and the inhibitory activity.

All these biological assays demonstrate that, like kynurenines **10a** and **10b**, the 4,5-dihydro-1*H*-pyrazole derivatives **11** could present neuroprotective properties through a nNOS inhibition mechanism. A comparison between both types of compounds could help to define a putative model for the interaction with nNOS.

The conformational behavior of kynurenines **10a** and **10b** has been described previously,[43] indicating the existence of several conformers that can be classified in two conformational families. One of this families is characterized by the presence of an intramolecular hydrogen bond between the 2′-NH_2 and the side chain carbonyl group and contains the more stable conformers of the molecule. In the other family such a hydrogen bond is not present and contains the more energetic conformations.

To find the similarities between compounds **10** and **11**, we have compared all the conformations of kynurenine derivatives with the four conformers found for each pyrazole compound, using a small Sybyl SPL program written for this purpose. This program scans both databases containing the corresponding conformers of each compound and superimposes each conformation of the first molecule over each conformation of the second one, using a selected set of atoms for both compounds (matching process). Simultaneously, in the superimposed conformations, the macro calculates the RMSD value between the coordinates of another selected set of atoms defined for each molecule (fitting process). When appropriated atoms are defined in the fitting process, the RMSD value is a good measure of the similarity between the relative spatial position of the pharmacophoric groups of both compounds.

The importance of the 2′-NH_2 group in the pharmacophore of kynurenines has been mentioned previously.[42,43] Since the nitrogen atom of the amide group acts as hydrogen bond donor in kynurenines and as an acceptor in pyrazolines, we have considered that this nitrogen is not a common pharmacophoric feature. Instead of that, the terminal carbonyl group could acts as a hydrogen bond acceptor and probably behaves in a similar way in both types of molecules on interacting with the enzyme. Finally, the benzene ring is also a common structural template for both families of compounds.

For these reasons, in the matching process we have chosen the benzene ring, the N atom of the 2′-NH_2 group and the carbon atom directly joined to the benzene ring in order to superimpose both compounds. In the fitting process, the benzene ring, the 2′-NH_2 group, and the amide oxygen atom have been selected as potential pharmacophoric groups. Using this procedure, we have found two conformations of kynurenines that fitted very well (RMSD = 0.4 Å) over the conformer **I** of pyrazole derivatives, and both conformations belong to the kynurenine conformational family with the intramolecular hydrogen bond.

Figure 3 shows the superimposition of compounds **10a** and **11o,** as an example. It can be seen that the relative energy of both conformations of compound **10a** is small (1.40 and 4.30 kcal/mol, respectively), and hence **10a** could easily adopt each one of these conformations. The main difference between both conformers is the relative orientation of the terminal methyl group. While in the more stable conformer of compound **10a** the methyl group points out at an opposite direction in relation to the methyl group of the pyrazole **11o** (Figure 3, left); in

the second conformer the methyl group of **10a** has a similar orientation to that of **11o** (Figure 3, right).

In the kynurenine family, substitution of the methyl group (**10a**) by a propyl (**10b**) decreases the nNOS inhibitory effect from 68.5% to 45.1%. Nevertheless, in the pyrazole derivatives, substitution of the methyl group by a more bulky one increases the nNOS inhibitory effect. Therefore, it seems clear that in the interaction with nNOS the methyl group of both types of compounds interact with different residues, and it can be concluded that the first superimposition is probably the correct one.

If we accept these findings as correct, a scheme for the interaction could be drawn (Figure 3) and summarized as follow:

(a) A pocket in the enzyme that accommodates the benzene rings present in kynurenines and pyrazoles (red arc). Substitution of 5′H (series B) by OMe (series A) or Cl (series C) increases the inhibitory activity in practically all compounds, and the electronic nature of the 5′-substituent (MeO, Cl, H) seems to be important for the biological activity. Nevertheless, the influence of the substituent is not absolutely clear, and it cannot be decided what is the main type of interaction (hydrophobic or electronic) with this part of the enzyme. Probably both types should be important.

(b) A hydrogen acceptor residue for the interaction with the free NH bond of the 2′-NH_2 group (blue arrow). Formation of this hydrogen bond has proven to be necessary since in the kynurenine family, elimination, monoalkylation, or bialkylation of the 2′-NH_2 group arises in a lack of nNOS inhibitory activity.[43]

(c) A hydrogen bond donor residue that can interacts with the amide oxygen atom of both kynurenine and pyrazole derivatives (red arrow). Both oxygen atoms match very well in the superimposed structures and has the same character as hydrogen bond acceptors.

(d) The R_2 substituent is accommodated in two different and near zones of the binding pocket. Since an increment in the R_2 volume in kynurenines provokes a decrease in activity, these molecules must orientate the R_2 substituent to a region with a small steric tolerance. On the contrary, the R_2 substituent in pyrazole must be orientated to a zone sterically allowed.

Conclusions

A new class of nNOs inhibitors have been designed, synthesized, and tested. These new compounds can be considered as rigid analogues of the previously described kynurenine derivatives **10** that also acts as nNOS inhibitors. Neither compound **10** nor **11** shows any inhibitory activity against the kynurenine 3-hydroxylase (KYN3OH), and, hence, the potential neuroprotective activity is only due to the nNOs inhibition.

Our experimental results and theoretical studies demonstrate the importance of the 2′-NH_2 substituent for the interaction with nNOS in both types of compounds since this group is necessary in the restriction of the conformational mobility of the molecule and in the formation of a hydrogen bond with the enzyme.

The conformational study indicates that low energy conformations of both types of molecules can be fitted with a low RMSD value for the benzene ring, the NH_2 group, and the oxygen atom of the carbonyl moiety. In the superimposed conformations, the orientation of the R_2 group is different in both types of structures, and this can be the reason for the different influence of R_2 over the inhibitory activity.

Finally, a higher increment in the activity would be expected from the conformational restriction of kynurenines, and this increment is not observed. This fact can be due to two reasons. The first one is that the kynurenine active conformation is different from that proposed in our interaction model and could not be properly mimicked by the pyrazole derivatives. The second possibility is that, even if the active conformation is mimicked by the pyrazole, other groups present in the molecules interact in a different way with the enzyme. In our model, the different orientation of R_2 in both families of compound could also explain why the expected high activity increment is not observed. Our model for the interaction with nNOS justifies the structure−activity relationships observed at the moment for both types of molecules, and this model could serve as a template for the design of other potential nNOS inhibitors.

Experimental Section

Melting points were determined in open capillaries using an Electrothermal-1A-6301 apparatus and are uncorrected. ^{1}H NMR and ^{13}C NMR spectra were recorded on a Bruker AMX 300 spectrometer operating at 75.479 MHz for ^{13}C NMR and 300.160 for ^{1}H in $CDCl_3$ and on a Bruker ARX 400 spectrometer operating at 400.132 MHz for ^{1}H and 100.623 MHz for ^{13}C (at concentration of ca. 27 mg mL^{-1} in all cases). The center of each peak of $CDCl_3$ [7.26 ppm (^{1}H) and 77.0 ppm (^{13}C)] was used as internal references in a 5 mm ^{13}C/^{1}H dual probe (Wilmad, No. 528-PP). The temperature of the sample was maintained at 297 K. The peaks are reported in ppm (δ). High-resolution mass spectroscopy (HRMS) was carried out on a VG AutoSpec Q high-resolution mass spectrometer (Fisons Instruments). Elemental analyses were performed on a Perkin-Elmer 240 C and agreed with theoretical values within ±0.4%. Flash-chromatography was carried out using silica gel 60, 230−240 mesh (Merck), and the solvent mixture reported within parentheses was used as eluent.

Preparation of 1-Acyl-3-(2-nitro-5-substituted-phenyl)-4,5-dihydro-1*H*-pyrazoles, 16a−s. General Method. 2-Nitro-5-substituted-phenyl vinyl ketone **14a−c** (1.44 mmol) was added to a solution of 0.120 mL (2.45 mmol) of hydrazine monohydrate in ethanol (15 mL), and the mixture was refluxed during 3 h. After this period, the mixture was cooled, extracted with diethyl ether (4 × 10 mL), dried (Na_2SO_4), filtered, and concentrated to dryness. Without isolation, the pyrazoline was dissolved in dry CH_2Cl_2, and triethylamine (1.5 mmol) and acetic anhydride or the acyl chloride (1.44 mmol) were added at room temperature under nitrogen atmosphere. The reaction mixture was stirred for 3 h, filtered, and washed with H_2O, 10% HCl, 2M NaOH, H_2O, and brine. The organic phase was dried (Na_2SO_4) and filtered. Evaporation of the solvent rendered a residue that was purified by flash chromatography (ethyl acetate:hexane 1:4).

1-Acetyl-3-(5-methoxy-2-nitrophenyl)-4,5-dihydro-1*H*-pyrazole, 16a: (70%); mp. 195−199 °C; MS (LSIMS) *m/z* 286.080541 (M + Na)$^+$, calcd mass for $C_{12}H_{13}N_3O_4Na$ 286.080376 (deviation −0.6 ppm).

1-Propionyl-3-(5-methoxy-2-nitrophenyl)-4,5-dihydro-1*H*-pyrazole, 16b: (75%); mp 195−199 °C; MS (LSIMS) *m/z* 300.096034 (M + Na)$^+$, calcd mass for $C_{13}H_{15}N_3O_4Na$ 300.096026 (deviation 0.0 ppm).

1-Butyryl-3-(5-methoxy-2-nitrophenyl)-4,5-dihydro-1*H*-pyrazole, 16c: (73%); mp 131−134 °C; MS (LSIMS) *m/z* 314.111657 (M + Na)$^+$, calcd mass for $C_{14}H_{17}N_3O_4Na$ 314.111676 (deviation 0.1 ppm).

1-Pentanoyl-3-(5-methoxy-2-nitrophenyl)-4,5-dihydro-1*H*-pyrazole, 16d: (85%); mp 103−105 °C; MS (LSIMS) *m/z* 328.127455 $(M + Na)^+$, calcd mass for $C_{15}H_{19}N_3O_4Na$ 328.127326 (deviation −0.4 ppm).

1-Cyclopropanecarbonyl-3-(5-methoxy-2-nitrophenyl)-4,5-dihydro-1*H*-pyrazole, 16e: (80%); mp 145−147 °C; MS (LSIMS) *m/z* 312.096293 $(M + Na)^+$, calcd mass for $C_{14}H_{15}N_3O_4Na$ 312.096026 (deviation −0.9 ppm).

1-Cyclobutanecarbonyl-3-(5-methoxy-2-nitrophenyl)-4,5-dihydro-1*H*-pyrazole, 16f: (82%); mp 115−118 °C; MS (LSIMS) *m/z* 326.110794 $(M + Na)^+$, calcd mass for $C_{15}H_{17}N_3O_4Na$ 326.111676 (deviation 2.7 ppm).

1-Cyclopentanecarbonyl-3-(5-methoxy-2-nitrophenyl)-4,5-dihydro-1*H*-pyrazole, 16g: (70%); mp 101−104 °C; MS (LSIMS) *m/z* 340.1127606 $(M + Na)^+$, calcd mass for $C_{16}H_{19}N_3O_4Na$ 340.127326 (deviation −0.8 ppm).

1-Cyclohexanecarbonyl-3-(5-methoxy-2-nitrophenyl)-4,5-dihydro-1*H*-pyrazole, 16h: (90%); mp 88−91 °C; MS (LSIMS) *m/z* 354.142959 $(M + Na)^+$, calcd mass for $C_{17}H_{21}N_3O_4Na$ 354.142976 (deviation 0.0 ppm).

1-Benzoyl-3-(5-methoxy-2-nitrophenyl)-4,5-dihydro-1*H*-pyrazole, 16i: (90%.); mp 143−147 °C; MS (LSIMS) *m/z* 348.096116 $(M + Na)^+$, calcd mass for $C_{17}H_{15}N_3O_4Na$ 348.096026 (deviation −0.3 ppm).

1-Acetyl-3-(2-nitrophenyl)-4,5-dihydro-1*H*-pyrazole, 16j: (65%); mp 161−165 °C; MS (LSIMS) *m/z* 256.069896 $(M + Na)^+$, calcd mass for $C_{11}H_{11}N_3O_3Na$ 256.069811 (deviation −0.3 ppm).

1-Propionyl-3-(2-nitrophenyl)-4,5-dihydro-1*H*-pyrazole, 16k: (75%); mp 111−115 °C; MS (LSIMS) *m/z* 270.085735 $(M + Na)^+$, calcd mass for $C_{12}H_{13}N_3O_3Na$ 270.085461 (deviation −1.0 ppm).

1-Butyryl-3-(2-nitrophenyl)-4,5-dihydro-1*H*-pyrazole, 16l: (70%); mp 131−134 °C; MS (LSIMS) *m/z* 284.101081 $(M + Na)^+$, calcd mass for $C_{13}H_{15}N_3O_3Na$ 284.101111 (deviation 0.1 ppm).

1-Cyclopropanecarbonyl-3-(2-nitrophenyl)-4,5-dihydro-1*H*-pyrazole, 16m: (65%); mp 139−144 °C; MS (LSIMS) *m/z* 282.085496 $(M + Na)^+$, calcd mass for $C_{13}H_{13}N_3O_3Na$ 282.085461 (deviation −0.1 ppm).

1-Benzoyl-3-(2-nitrophenyl)-4,5-dihydro-1*H*-pyrazole, 16n: (90%); mp 108−113 °C; MS (LSIMS) *m/z* 318.085772 $(M + Na)^+$, calcd mass for $C_{16}H_{13}N_3O_3Na$ 318.085461 (deviation −1.0 ppm).

1-Acetyl-3-(5-chloro-2-nitrophenyl)-4,5-dihydro-1*H*-pyrazole, 16o: (60%); mp 208−211 °C; MS (LSIMS) *m/z* 268.048362 $(M + Na)^+$, calcd mass for $C_{11}H_{10}ClN_3O_3Na$ 268.048894 (deviation 2.0 ppm).

1-Propionyl-3-(5-chloro-2-nitrophenyl)-4,5-dihydro-1*H*-pyrazole, 16p: (50%); mp 142−147 °C; MS (LSIMS) *m/z* 304.046052 $(M + Na)^+$, calcd mass for $C_{12}H_{12}ClN_3O_3Na$ 304.046489 (deviation 1.4 ppm).

1-Butyryl-3-(5-chloro-2-nitrophenyl)-4,5-dihydro-1*H*-pyrazole, 16q: (55%); mp 104−110 °C; MS (LSIMS) *m/z* 318.061733 $(M + Na)^+$, calcd mass for $C_{13}H_{14}ClN_3O_3Na$ 318.062139 (deviation 1.3 ppm).

1-Cyclopropanecarbonyl-3-(5-chloro-2-nitrophenyl)-4,5-dihydro-1*H*-pyrazole, 16r: (55%); mp 115−121 °C; MS (LSIMS) *m/z* 316.046563 $(M + Na)^+$, calcd mass for $C_{13}H_{12}ClN_3O_3Na$ 316.046489 (deviation −0.2 ppm).

1-Benzoyl-3-(5-chloro-2-nitrophenyl)-4,5-dihydro-1*H*-pyrazole, 16s: (60%); mp 153−157 °C; MS (LSIMS) *m/z* 352.045827 $(M + Na)^+$, calcd mass for $C_{16}H_{12}ClN_3O_3Na$ 352.046489 (deviation 1.9 ppm).

Preparation of 1-Acyl-3-(2-amino-5-methoxyphenyl)-4,5-dihydro-1*H*-pyrazoles 11a−i and 1-Acyl-3-(2-aminophenyl)-4,5-dihydro-1*H*-pyrazoles, 11j−n. General Method. A mixture of nitroarene (414 mmol) and 10% Pd/C (10 mg) was dissolved in methanol and stirred under a hydrogen atmosfere (1 atm) for 3 h. The mixture was filtered through Celite, washed with H_2O (2 × 15 mL), dried, and evaporated to dryness.The yellow solid residue was recrystalized from CH_2Cl_2/hexane which afforded the aromatic amine. All compounds were obtained in quantitative yield.

1-Acetyl-3-(2-amino-5-methoxyphenyl)-4,5-dihydro-1*H*-pyrazole, 11a: mp 218−220 °C; MS (LSIMS) *m/z* 256.106034 $(M + Na)^+$, calcd mass for $C_{12}H_{15}N_3O_2Na$ 256.106197 (deviation 0.6 ppm). Anal. $C_{12}H_{15}N_3O_2$ (C, H, O).

1-Propionyl-3-(2-amino-5-methoxyphenyl)-4,5-dihydro-1*H*-pyrazole, 11b: mp 162−165 °C; MS (LSIMS) *m/z* 270.121809 $(M + Na)^+$, calcd mass for $C_{13}H_{17}N_3O_2Na$ 270.121847 (deviation 0.1 ppm). Anal. $C_{13}H_{17}N_3O_2$ (C, H, O).

1-Butyryl-3-(2-amino-5-methoxyphenyl)-4,5-dihydro-1*H*-pyrazole, 11c: mp 172−175 °C; MS (LSIMS) *m/z* 284.137695 $(M + Na)^+$, calcd mass for $C_{14}H_{19}N_3O_2Na$ 284.137497 (deviation −0.7 ppm). Anal. $C_{14}H_{19}N_3O_2$ (C, H, O).

1-Pentanoyl-3-(2-amino-5-methoxyphenyl)-4,5-dihydro-1*H*-pyrazole, 11d: mp 166−169 °C; MS (LSIMS) *m/z* 298.153349 $(M + Na)^+$, calcd mass for $C_{15}H_{21}N_3O_2Na$ 298.153147 (deviation −0.7 ppm). Anal. $C_{15}H_{21}N_3O_2$ (C, H, O).

1-Cyclopropanecarbonyl-3-(2-amino-5-methoxyphenyl)-4,5-dihydro-1*H*-pyrazole, 1e: mp 140−143 °C; MS (LSIMS) *m/z* 282.121782 $(M + Na)^+$, calcd mass for $C_{14}H_{17}N_3O_2Na$ 282.121847 (deviation 0.2 ppm). Anal. $C_{14}H_{17}N_3O_2$ (C, H, O).

1-Cyclobutanecarbonyl-3-(2-amino-5-methoxyphenyl)-4,5-dihydro-1*H*-pyrazole, 11f: mp 160−162 °C; MS (LSIMS) *m/z* 296.137761 $(M + Na)^+$, calcd mass for $C_{15}H_{19}N_3O_2Na$ 296.137497 (deviation −0.9 ppm). Anal. $C_{15}H_{19}N_3O_2$ (C, H, O).

1-Cyclopentanecarbonyl-3-(2-amino-5-methoxyphenyl)-4,5-dihydro-1*H*-pyrazole, 11 g: mp 160−162 °C; MS (LSIMS) *m/z* 310.153206 $(M + Na)^+$, calcd mass for $C_{16}H_{21}N_3O_2Na$ 310.153147 (deviation −0.2 ppm). Anal. $C_{16}H_{21}N_3O_2$ (C, H, O).

1-Cyclohexanecarbonyl-3-(2-amino-5-methoxyphenyl)-4,5-dihydro-1*H*-pyrazole, 11h: mp 144−147 °C; MS (LSIMS) *m/z* 324.169049 $(M + Na)^+$, calcd mass for $C_{17}H_{23}N_3O_2Na$ 324.168797 (deviation −0.8 ppm). Anal. $C_{17}H_{23}N_3O_2$ (C, H, O).

1-Benzoyl-3-(2-amino-5-methoxyphenyl)-4,5-dihydro-1*H*-pyrazole, 11i: mp 139−142 °C; MS (LSIMS) *m/z* 318.121816 $(M + Na)^+$, calcd mass for $C_{17}H_{17}N_3O_2Na$ 318.121847 (deviation 0.1 ppm). Anal. $C_{17}H_{17}N_3O_2$ (C, H, O).

1-Acetyl-3-(2-aminophenyl)-4,5-dihydro-1*H*-pyrazole, 11j: mp 220−224 °C; MS (LSIMS) *m/z* 226.095741 $(M + Na)^+$, calcd mass for $C_{11}H_{13}N_3ONa$ 226.095632 (deviation −0.5 ppm). Anal. $C_{11}H_{13}N_3O$ (C, H, O).

1-Propionyl-3-(2-aminophenyl)-4,5-dihydro-1*H*-pyrazole, 11k: mp 162−166 °C; MS (LSIMS) *m/z* 240.111073 $(M + Na)^+$, calcd mass for $C_{12}H_{15}N_3ONa$ 240.111007 (deviation 0.9 ppm). Anal. $C_{12}H_{15}N_3O$ (C, H, O).

1-Butyryl-3-(2-aminophenyl)-4,5-dihydro-1*H*-pyrazole, 11*l*: mp 146−151 °C; MS (LSIMS) *m/z* 254.126751 $(M + Na)^+$, calcd mass for $C_{13}H_{17}N_3ONa$ 254.126932 (deviation 0.7 ppm). Anal. $C_{13}H_{17}N_3O$ (C, H, O).

1-Cyclopropanecarbonyl-3-(2-aminophenyl)-4,5-dihydro-1*H*-pyrazole, 11m: mp 154−158 °C; MS (LSIMS) *m/z* 252.111155 $(M + Na)^+$, calcd mass for $C_{13}H_{15}N_3ONa$ 252.111282 (deviation 0.5 ppm). Anal. $C_{13}H_{15}N_3O$ (C, H, O).

1-Benzoyl-3-(2-aminophenyl)-4,5-dihydro-1*H*-pyrazole, 11n: mp 124−127 °C; MS (LSIMS) *m/z* 266.128979 $(M + H)^+$, calcd mass for $C_{16}H_{16}N_3O$ 266.129337 (deviation 1.3 ppm). Anal. $C_{16}H_{15}N_3O$ (C, H, O).

Preparation of 1-Acyl-3-(2-amino-5-chlorophenyl)-4,5-dihydro-1*H*-pyrazoles, 11o−s. General Method. A mixture of nitroarene (487 mmol) and $SnCl_2$ (440 mg) was dissolved in ethanol and was stirred under reflux for 1 h. The solution was quenched to pH = 7 with sat. $NaHCO_3$, extracted with ethyl acetate (2 × 15 mL), and dried (Na_2SO_4). Evaporation of the solvent gave a yellow solid residue which was recrystallized from CH_2Cl_2/hexane. The aromatic amines wer obtained in quantitative yield.

1-Acetyl-3-(2-amino-5-chlorophenyl)-4,5-dihydro-1*H*-pyrazole, 11o: mp 261−266 °C; MS (LSIMS) *m/z* 260.056192 $(M + Na)^+$, calcd mass for $C_{11}H_{12}ClN_3ONa$ 260.056660 (deviation 1.8 ppm). Anal. $C_{11}H_{12}ClN_3O$ (C, H, O).

1-Propionyl-3-(2-amino-5-chlorophenyl)-4,5-dihydro-1*H*-pyrazole, 11p: mp 238−243 °C; MS (LSIMS) *m/z* 274.072808 $(M + Na)^+$, calcd mass for $C_{12}H_{14}ClN_3ONa$ 274.072310 (deviation −1.8 ppm). Anal. $C_{12}H_{14}ClN_3O$ (C, H, O).

1-Butyryl-3-(2-amino-5-chlorophenyl)-4,5-dihydro-1*H*-pyrazole, 11q: mp 216−220 °C; MS (LSIMS) *m/z* 288.088141 $(M + Na)^+$, calcd mass for $C_{13}H_{16}ClN_3ONa$ 288.087960 (deviation −0.6 ppm). Anal. $C_{13}H_{16}ClN_3O$ (C, H, O).

1-Cyclopropanecarbonyl-3-(2-amino-5-chlorophenyl)-4,5-dihydro-1*H*-pyrazole, 11r: mp 218−222 °C; MS (LSIMS) *m/z* 286.072010 $(M + Na)^+$, calcd mass for $C_{13}H_{14}ClN_3O$ 286.072310 (deviation 1.0 ppm). Anal. $C_{13}H_{16}ClN_3O$ (C, H, O).

1-Benzoyl-3-(2-amino-5-chlorophenyl)-4,5-dihydro-1*H*-pyrazole, 11s: mp 155−158 °C; MS (LSIMS) *m/z* 322.071949 $(M + Na)^+$, calcd mass for $C_{16}H_{14}ClN_3ONa$ 322.072310 (deviation 1.1 ppm). Anal. $C_{16}H_{14}ClN_3O$ (C, H, O).

Computational Methodology. Conformational analysis of studied compounds has been performed using the Tripos[46] force field, implemented in the Sybyl[48] modeling program. Initial geometries have been generated from fragments defined in the standard libraries of the program and have been optimized using the Powell[49] method until the energy gradient drops below 0.01 kcal/mol Å^2. Electrostatic energy has been calculated from the partial atomic charges generated by the Gasteiger[50] method, using a distance-dependent dielectric constant equal to one ($\epsilon = 1$).

After the initial optimization, a conformational search of each compound using the Sybyl Gridsearch utility has been performed in order to locate the most stable conformer. With this purpose, all side chain rotatable bonds as well as the bond that joined both rings have been rotated using an interval of 30°; and the resulting conformations have been optimized after elimination of all the constrains. The comparison of all the optimized conformers each other allows to identify those that are energetically and geometrically unique.

Striatal nNOS Activity Determination. L-Arginine, L-citruline, *N*-(2-hydroxymethyl)piperazine-*N*′-(2-ethanesulfonic acid) (HEPES), DL-dithiothreitol (DTT), leupeptin, aprotinin, pepstatin, phenylmethylsulfonylfluoride (PMSF), hypoxantine-9-β-D-ribofuranosid (inosine), ethylene glycol-bis(2-aminoethyl ether)-*N*,*N*,*N*′,*N*′-tetraacetic acid (EGTA), bovine serum albumin (BSA), Dowex-50 W (50 × 8-200), FAD, NADPH, and 5,6,7,8-tetrahydro-L-biopterin dihydrocloride (H_4-biopterin) were obtained from Sigma-Aldrich Química (Spain). L-[^{3}H]-Arginine (58 Ci/mmol) was obtained from Amersham (Amersham Biosciences, Spain). Tris(hydroxymethyl)aminomethane (Tris-HCl) and calcium chloride were obtained from Merck (Spain).

The rats were killed by cervical dislocation, and the striata were quickly collected and immediately used to measure NOS activity. Upon removal, the tissues were cooled in ice-cold homogenizing buffer (25 mM Tris, 0.5 mM DTT, 10 μg/mL leupeptin, 10 μg/mL pepstatine, 10 μg/mL aprotinine, 1 mM PMSF, pH 7.6). Two striata were placed in 1.25 mL of the same buffer and homogenized in a Polytron (10 s × 6). The crude homogenate was centrifuged for 5 min at 1000*g*, and aliquots of the supernatant were either stored at −20 °C for total protein determination[51] or used immediately to measure NOS activity. The nNOS activity was measured by the Bredt and Snyder[52] method, monitoring the conversion of L-[^{3}H]-arginine to L-[^{3}H]-citruline. The final incubation volume was 100 μL and consisted of 10 μL of crude homogenate added to a buffer to give a final concentration of 25 mM Tris, 1 mM DTT, 30 μM H_4-biopterin, 10 μM FAD, 0.5 mM inosine, 0.5 mg/mL BSA, 0.1 mM $CaCl_2$, 10 μM L-arginine, and 50 nM L-[^{3}H]-arginine, at pH 7.6. The reaction was started by the addition of 10 μL of NADPH (0.75 mM final) and 10 μl of each pyrazole derivative in DMSO to give a final concentration of 1 mM. The tubes were vortex and incubated at 37 °C for 30 min. Control incubations were performed by the omission of NADPH. The reaction was halted by the addition of 400 μL of cold 0.1 M HEPES, 10 mM EGTA, and 0.175 mg/mL L-citruline, pH 5.5. The reaction mixture was decanted into a 2 mL column packet with Dowex-50 W ion-exchange resin (Na^+ form) and eluted with 1.2 mL of water. L-[^{3}H]-Citruline was quantified by liquid scintillation spectroscopy. The retention of L-[^{3}H]-arginine in this process was greater than 98%. Specific enzyme activity was determined by subtracting the control value, which usually amounted to less than 1% of the radioactivity added. The nNOS activity was expressed as picomoles of l-[^{3}H]-citruline produced (mg of protein)$^{-1}$ min^{-1}.

Striatal KYN3OH Activity Determination. L-Kynurenine, 3-hydroxykynurenine, sucrose, NADPH, DHBA, DMSO, perchloric acid, triethylamine, phosphoric acid, heptanesulfonic acid, and EDTA-Na_2 were obtained from Sigma-Aldrich (Spain). HPLC-grade acetonitrile was obtained from Panreac (Spain). The water used for the preparation of solutions was of Milli-RO/Q grade (Millipore Iberica, Spain). All remaining chemicals were of analytical grade and were purchased from Sigma-Aldrich (Spain).

Tissue for KYN3OH determination was prepared from rats after being killed by cervical dislocation. Striata were rapidly removed, washed in cold saline, homogenized in 8 vol of sucrose 0.31 M, and centrifuged at 10000*g* for 30 min at 4 °C. The pellets were rinsed in sucrose 0.32 M and centrifuged twice. The obtained pellets were resuspended in 8 vol of 0.14 M KCl, 20 mM phosphate buffer, pH 7, and frozen to −20 °C until the assay.

The KYN3OH activity was measured following the Carpenedo[53] method, monitoring the conversion of L-kynurenine to 3-hydroxykynurenine. The final incubation volume was 120 μL and consisted in 100 μL of crude homogenate added to the buffer to give a final concentration of 0.1 M phosphate, 4 mM $MgCl_2$, and 100 μM L-kynurenine. This solution was completed with 10 μL of 40 mM NADPH and 10 μL of each pyrazole derivative at a final concentration of 1 mM in DMSO. The tubes were vortex and incubated at 37 °C for 60 min. The reaction was stopped, placing the tubes on ice and adding 100 μL of cold 1 M perchloric acid. To this mixture was added 10 μL of DHBA as internal standard, and the samples were centrifuged at 12000*g* for 10 min at 4 °C. The supernatant were removed and frozen to −20 °C until 3-hydroxykynurenine determination. The concentration of 3-hydroxykynurenine was quantified by HPLC with electrochemical detection, following the method of Heyes and Quearry[54] with slight modifications. Separation was done in a C-18 reversed-phase 3 μm sphere analytical column. The applied potential was set at +0.6 V using a glass carbon electrode versus an Ag/AgCl reference electrode. The mobile phase consisted of 20 mL of acetonitrile, 9 mL of triethylamine, 5.9 mL of phosphoric acid, 100 mg of EDTA-Na_2, and 1.8 g of heptaneosulfonic acid in 1000 mL of deionized water. The solution was filtered through a 0.45 μm filter and degassed before use. Analyses were done at a flow rate of 1 mL/min at room temperature. The concentration of 3-hydroxykynurenine was calculated using DHBA as internal standard and a calibration curve obtained from the corresponding standard injected in the HPLC system. The calculated concentration is expressed as nmol/h/g wet brain.

Statistical Analysis. Data are expressed ad the mean ± SD. One-way analysis of variance, followed by the Newman-Keuls multiple range test was used. A $P < 0.05$ value was considered statistically significant.

Acknowledgment. This work was partially supported by grants from the Ministerio de Ciencia y Tecnología (SAF2002-01688) and from the Fondo de Investigación Sanitaria (PI021181 and PI02/1447).

Supporting Information Available: Spectroscopic data (^{1}H and ^{13}C NMR) of compounds **11a**−**s** and **16a**−**s** and elemental analyses data for **11a**−**s**. This material is available free of charge via the Internet at http://pubs.acs.org.

References

(1) Danbolt, N. C. Glutamate uptake. *Prog. Neurobiol*. **2001**, *65*, 1−105.
(2) Dingledine, R.; Borges, K.; Bowie, D.; Traynelis, S. F. The glutamate receptor ion channels. *Pharmacol. Rev*. **1999**, *51*, 7−61.
(3) Herrling, P. L. Clinical implications of NMDA receptors. In *The NMDA receptor*; Colingridge, G. L.; Watkins, J. C., Eds.; Oxford: Oxford University Press, 1994; pp 376−394.

(4) Meldrum, B.; Garthwaite, J. Excitatory amino acid neurotoxicity and neurodegenerative diseases. *Trends Pharmacol. Sci.* **1990**, *11*, 379−387.
(5) Sattler, R.; Tymianski, M. Molecular mechanisms of calcium-dependent excitotoxicity. *J. Mol. Med*. **2000**, *78*, 3−13.
(6) Schwarcz, R. Metabolism and function of brain kynurenines. *Biochem. Soc. Trans*. **1993**, *21*, 77−82.
(7) Swartz, K. J.; During, M. J.; Freese, A.; Beal, M. F. Cerebral synthesis and release of kynurenic acid: an endogenous antagonist of excitatory amino acid receptors. *J. Neurosci*. **1990**, *10*, 2965−2973.
(8) Stone, T. W.; Perkins, M. N. Quinolinic acid: a potent endogenous excitant at amino acid receptors in rat CNS. *Eur. J. Pharmacol*. **1981**, *72*, 411−412.
(9) Meldrum, B. S.; Chapman, A. G. Competitive NMDA antagonist as drugs. In *The NMDA receptor*; Colingridge, G. L.; Watkins, J. C., Eds.; Oxford: Oxford University Press, 1994; pp 376−394.
(10) Schwarcz, R.; Foster, A. C.; French, E. D.; Whetsell, W. O.; Köhler, C. Excitotoxic models for neurodegenerative disorders. *Life Sci*. **1984**, *35*, 19−32.
(11) Beal, M. F.; Kowall, N. W.; Ellison, D. W.; Mazurek, M. F.; Swartz, K. J.; Martin, J. B. Replication of the neurochemical characteristics of Huntington's disease by quinolinic acid. *Nature* **1986**, *321*, 168−171.
(12) Kerr, S. J.; Armati, P. J.; Brew, B. J. Neurotoxicity of quinolinic acid in human brain cultures. *J. Neurovirol.* **1995**, *1*, 375−238.
(13) Heyes, M. P.; Saito, K.; Lackner, A.; Wiley, A.; Achim, C. L.; Markey, S. P. Sources of the neurotoxin quinolinic acid in the brain of HIV-1 infected patients and retrovirus-infected macaques. *FASEB J*. **1988**,*12*, 881−896.
(14) Santamaría, A.; Galvan-Arzate, S.; Lysy, V. Quinolinic acid induces oxidative stress in rat brain synaptosomes. *Neuroreport* **2001**, *12*, 871−874.
(15) Santamaría, A.; Jiménez-Capdevilla, M. E.; Camacho, A.; Rodríguez-Martínez, E.; Flores, A.; Galván-Arzate, S. In vivo hydroxyl radical formation after quinolinic acid infusion into rat corpus striatum. *Neuroreport* **2001**, *12*, 2693−2696.
(16) Bordelon, Y. M.; Chesselet, M. F.; Nelson, D.; Welsch, F. Erecinska, M. Energetic disfunction in quinolinic acid-lesioned rat striatum. *J. Neurochem.* **1997**, *69*, 1629−1639.
(17) Birch, P. J.; Grossman, C. J.; Hayes, A. G. Kynurenic acid antagonises responses to NMDA via an action at the strychnine-insensitive glycine receptor. *Eur. J. Pharmacol*. **1988**, *1*, 85−87.
(18) Parsons, C. G.; Danysz, W.; Quack, G.; Hartmann, S.; Lorenz, B.; Wollenburg, C.; Baran, L.; Przegalinski, E.; Kostowski, W.; Krzascik, P.; Chizh, B.; Headley, P. M. Novel systemically active antagonists of the glycine site of the *N*-methyl-D-aspartate receptor: electrophysiological, biochemical and behavioral characterization. *J. Pharmacol. Exp. Ther*. **1997**, *3*, 1264−1275.
(19) Foster, A. C.; Vezzani, A.; French, E. D.; Schwarcz, R. Kynurenic acid blocks neurotoxicity and seizures induced in rats by the related brain metabolite quinolinic acid. *Neurosci Lett*. **1984**, *3*, 273−278.
(20) Saito, K.; Nowak, T. S., Jr.; Markey, S. P.; Heyes, M. P. Mechanism of delayed increases in kynurenine pathway metabolism in damaged brain regions following tansient cerebral ischemia. *J. Neurochem*. **1993**, *60*, 180−182.
(21) Moroni, F. Tryptophan metabolism and brain function: focus on kynurenine and other indole metabolites. *Eur. J. Pharmacol*. **1999**, *375*, 87−100.
(22) Kemp, J. A.; Foster, A. C.; Leeson, P. D.; Priestly, T.; Tridgett, R.; Iversen L. L.; Woodruff, G. N. 7-Chlorokynurenic acid is a selective antagonist at the glycine modulatory site of the *N*-methyl-D-aspartate receptor complex. *Proc. Natl. Acad. Sci. U.S.A.* **1988**, *85*, 6547−6550.
(23) (a) McNamara, D.; Smith, E. C.; Calligaro, D. O.; O'Malley, P. J.; McQuaid, L. A.; Dingledine, R. 5,7-Dichlorokynurenic acid, a potent and selective competitive antagonist of the glycine site on NMDA receptors. *Neurosci Lett.* **1990**, *120*, 17−20. (b) Baron, B. M.; Harrison, B. L.; Miller, F. P.; McDonald, I. A.; Salituro, F. G.; Schmidt, C. J.; Sorensen, S. M.; White, H. S.; Palfreyman, M. G. Activity of 5,7-dichlorokynurenic acid, a potent antagonist at the *N*-methyl-D-aspartate receptor-associated glycine binding site. *Mol. Pharmacol*. **1990**, *38*, 554−561.
(24) Takano, K.; Tatlisumak, T.; Formato, J. E.: Carano, R. A.; Bergmann, A. G.; Pullan, L. M.; Bare, T. M.; Sotak, C. H.; Fisher, M. Glycine site antagonist attenuates infarct size in experimental focal ischemia. Postmortem and diffusion mapping studies. *Stroke* **1997**, *28*, 1255−1262.
(25) Stone, T. W.; Darlington, L. G. Endogenous kynurenines as targets for drug discovery and development. *Nat. Rev. Drug Discov*ery **2002**, *1*, 609−620.
(26) a) Stone, T. W. Kynurenic acid antagonists and kynurenine pathway inhibitors. *Expert Opin. Investig. Drugs* **2001**, *10*, 633−645. (b) Stone, T. W. Kynurenines in the CNS: from endogenous obscurity to therapeutic importance. *Prog. Neurobiol*. **2001**, *64*, 185−218.
(27) Moroni, F.; Russi, P.; Gallo-Mezo, M. A.; Moneti, G.; Pellicciari, R. Modulation of quinolinic and kynurenic acid content in the rat brain: effects of endotoxins and nicotinylalanine. *J. Neurochem*. **1991**, *57*, 1630−1635.
(28) (a) Connick, J. H.; Heywood, G. C.; Sills, G. J.; Thompson, G. G.; Brodie, M. J.; Stone, T. W. Nicotinylalanine increases cerebral kynurenic acid content and has anticonvulsant activity. *Gen. Pharmacol*. **1992**, *23*, 235−239. (b) Russi, P.; Alesiani, M.; Lombardi, G.; Davolio, P.; Pellicciari, R.; Moroni, F. Nicotinylalanine increases the formation of kynurenic acid in the brain and antagonizes convulsions. *J. Neurochem*. **1992**, *59*, 2076−2080.
(29) Schwarcz, R.; Pellicciari, R. Manipulation of brain kynurenines: glial targets, neuronal effects, and clinical opportunities. *J. Pharmacol. Exp. Ther*. **2002**, *303*, 1−10.
(30) Moncada, S.; Palmer, R. M. J.; Higgs, E. A. Nitric Oxide: Physiology, Pathophysiology, and Pharmacology. *Pharmacol. Rev*. **1991**, *43*, 109−142.
(31) Mayer, B. M.; John, M.; Bohme, E. Purification of a Ca2+/Calmodulin-Dependent Nitric Oxide Synthase from Porcine Cerebellum: Cofactor Role of Tetrahydrobiopterin. *FEBS. Lett.* **1990**, *277*, 215−219.
(32) Pollock, J. S.; Förstermann, U.; Mitchel, J. A.; Warner, T. D.; Schmidt, H. H.; Nakane, M.; Murad, F. Purification and Characterization of Particulate Endothelium Derived Relaxing Factor Synthase from Cultured and Native Bovine Aortic Endothelial Cells. *Proc. Natl. Acad. Sci. U.S.A.*. **1991**, *88*, 10480−10484.
(33) Stuehr, D. J.; Cho, H. J.; Kwon, N. S.; Weise, M. F.; Nathan, C. F. Purification and Characterization of the Cytokine-Induced Macrophage Nitric Oxide Synthase: a FAD-Containing and FMN-Containing Flavoproteins. *Proc. Natl. Acad. Sci. U.S.A.* **1991**, *88*, 7773−7777.
(34) Hevel, J. M.; White, K. A.; Marletta, M. A. Purification of the Inducible Murine Macrophage Nitric Oxide Synthase. Identification as a Flavoprotein. *J. Biol. Chem*. **1991**, *266*, 22789−22791.
(35) Knowles, R. G.; Palacios, M.; Palmer, M. R. J.; Moncada, S. Formation of Nitric Oxide from L-Arginine in the Central Nervous System: A Transduction Mechanism for Stimulation of the Soluble Guanylate Cyclase. *Proc. Natl. Acad. Sci. U.S.A.* **1989**, *86*, 5159−5162.
(36) McCall, T. B.; Boughton-Smith, N. K.; Palmer, R. M. J.; Whittle, B. J. R.; Moncada, S. Synthesis of Nitric Oxide from L-arginine by Neutrophils: Release and Interaction with Superoxide Anion. *Biochem. J*. **1989**, *261*, 293−296.
(37) Pozo, D., Osuna, C., Calvo, J. R., Guerrero, J. M.: Produccion de Oxido Nitrico y Su Modulacion en el Sistema Inmune y el Sistema Nervioso. Archivos de Neurociencias. *Arch. Neurocien*. **1998**, *3*, 84−94.
(38) Smith, M. A.; Vasak, M.; Knipp, M.; Castellani, R. J.; Perry, G. Dimethylargininase, a nitric oxide protein, in Alzheimer disease. *Free Radical Biol. Med.* **1998**, *25*, 898−902.
(39) Yew, D. T.; Wong, H. W.; Li, W. P.; Lai, H. W.; Yu, W. H. Nitric oxide synthase in different areas of normal aged and Alzheimer's brains. *Neuroscience* **1999**, *89*, 675−686.
(40) Wong, N. K.; Strong, M. J. Nitric oxide synthase expression in cervical spinal cord in sporadic amyotrophic lateral sclerosis. *Eur. J. Cell. Biol.* **1998**, *77*, 338−343.
(41) Norris, P. J.; Waldvogel, H. J.; Faull, R. L.; Love, D. R.; Emson, P. C. Decreased neuronal nitric oxide synthase messenger RNA and somatostatin messenger RNA in the striatum of Huntington's disease. *Neuroscience* **1996**, *4*, 1037−1047.
(42) León, J.; Vives, F.; Crespo, E.; Camacho, E.; Espinosa, A., Gallo, M. A.; Escames, G.; Acuña-Castroviejo, D. Modification of Nitric Oxide Synthase Activity and Neuronal Response in Rat Striatum by Melatonin and Kynurenine Derivates. *J. Neuroendocrinol*. **1998**, *10*, 297−302.
(43) Camacho, E.; León, J.; Carrión, A.; Entrena, A.; Escames, G.; Khaldy, H.; Acuña-Castroviejo, D.; Gallo, M. A.; Espinosa, A. Inhibition of nNOS Activity in Rat Brain by Synthetic Kynurenines: Structure−Activity Dependence. *J. Med. Chem.* **2002**, *45*, 263−274.
(44) Fürstner, A.; Jumbam, D.; Scidel, G. Syntheses of zindoxifene and analogues by titanium-induced oxo-amide cupling. *Chem. Ber*. **1994**, *127*, 1125−1130.
(45) Shen, W.; Coburn, C. A.; Bornmann, W. G.; Danishefsky, S. J. Concise total syntheses of dl-camptothecin and related anticancer drugs. *J. Org. Chem*. **1993**, *58*, 611−617.
(46) Clark, M.; Cramer, R. D.; Van Opdenbosch, N. Validation of the general-purpose tripos 5.2 force-field. *J. Comput. Chem*. **1989**, *10*, 982−1012.
(47) Frisch, M. J.; Trucks, G. W.; Schlegel, H. B.; Gill, P. M. W.; Jonson, B. G.; Robb, M. A.; Cheseman, J. R.; Keith, T.; Peterson, G. A.; Montgomery, J. A.; Raghavachari, K.; Al-Laham, M. A.; Zakrzewski, V. G.; Ortiz, J. V.; Foresman, J. B.; Cioslowski, J.; Stefanov, B. B.; Nanayakkara, A.; Challacombe, M.; Peng, C.

Y.; Ayala, P. Y.; Chen, W.; Wong, M. W.; Andres, J. L.; Replogle, E. S.; Gomperts, R.; Martin, R. L.; Fox, D. J.; Binkley, J. S.; Defrees, D. J.; Baker, J.; Stewart, J. P.; Head-Gordon, M.; Gonzalez, C.; Pople, J. A. Gaussian, Inc., Pittsburgh, PA, 1995.

(48) SYBYL Molecular Modeling Software, Tripos Inc. 1699 S. Hanley Rd, St. Louis, MO 63144-2913; www.tripos.com.

(49) Powell, M. J. D. Restart Procedures for the Conjugate Gradient Method. *Math. Program.* **1997**, *12*, 241−254.

(50) (a) Gasteiger, J.; Marsili, M. Iterative Partial Equalization of Orbital Electronegativity. A Rapid Access to Atomic Charges. *Tetrahedron*, **1980**, *36*, 3219−3228. (b) Marsili, M.; Gasteiger, J. Charge Distributions from Molecular Topology and Pi-orbital Electronegativity. *Croat. Chem. Acta*. **1980**, *53*, 601−614. (c) Gasteiger, J.; Marsili, M. Prediction of Proton Magnetic Resonance Shifts: The Dependence on Hydrogen Charges Obtained by Iterative Partial Equalization of Orbital Electronegativity. *Org. Magn. Reson*. **1981**, *15*, 353−360.

(51) Lowry, O. H.; Rosebroigh N. J.; Farr, A. S.; Randall, R. J. Protein measurement with the Folin Phenol reagent. *J. Biol. Chem*. **1951**, *193*, 265−267.

(52) Bredt, D. S.; Snyder, S. H. Isolation of Nitric Oxide Synthethase, a Calmodulin Requiring Enzyme. *Proc. Natl. Acad. Sci. U.S.A.* **1990**, *87*, 682.

(53) Carpenedo, R.; Chiarugi, A.; Russi, P.; Lombardi, G.; Carla, V.; Pellicciari, R.; Mattoli, L.; Moroni, F. Inhibitors of kynurenine hydroxylase and kynureninase increase cerebral formation of kynurenate and have sedative and anticonvulsant activities. *Neuroscience* **1994**, *61*, 237−243.

(54) Heyes, M. P.; Quearry, B. J. Quantification of 3-hydroxykynurenine in brain by high-perfomance liquid chromatography and electrochemical detection. *J. Cromatogr*. **1988**, *428*, 340−344.

JM0407714